

OLD AND NEW COCHLEAR MAPS

Reinhart Frosch

Sommerhaldenstrasse 5B, CH-5200 Brugg, Switzerland; reinifrosch@bluewin.ch
PSI (Paul Scherrer Institute), Villigen and ETH (Eidgenössische Technische Hochschule), Zurich (retired)

1. INTRODUCTION

In the mammalian-cochlea literature there are two “old” categories of cochlear maps (i.e., curves of frequency f versus distance x from the base), namely the passive-peak (PP) and the low-level active-peak (AP) maps; the AP frequency is often denoted as “characteristic frequency”. At given x , the PP map indicates the frequency yielding the maximal basilar-membrane (BM) velocity amplitude in a cochlea without viable outer hair-cells (OHC) or, approximately, in a healthy cochlea at sound-pressure levels (SPL) of about 100 dB. The AP map indicates, at given x in a healthy cochlea, the frequency yielding the maximal BM velocity amplitude at SPL below about 20 dB. At given $x < 0.3L$ (where L is the total BM length) the AP frequency is found to be higher than the PP frequency by about 0.5 octave (i.e., by a frequency factor of $R = f_{AP} / f_{PP} = 2^{0.5} \approx 1.4$); see Fig. 1 below.

In the two just mentioned SPL regions (i.e., at <20 dB and at ~ 100 dB) the BM velocity v_{BM} at given place x and frequency f is found to be proportional to the sound pressure in the ear canal (EC). It is assumed that also the corresponding sound-pressure difference δp between two points, at the given x , just “above” and just “below” the BM in a two-dimensional cochlear model is proportional to the EC sound pressure. Then a complex specific acoustical BM impedance $Z_{BM} = \delta p / v_{BM}$ can be defined. At given frequency $f > f_{AP}(x = 0.3L)$, impedance functions $Z_{BM}(x)$ such as that shown in Fig. 2 below have been derived from experiments; see de Boer (2006).

In the present study, two “new” categories of cochlear maps related to the just discussed impedance function $Z_{BM}(x, f)$ are presented. In a passive cochlea, that function is related to the angular frequency $\omega = 2\pi f$ and to the BM properties as follows [see e.g. de Boer (1996)]:

$$Z_{BM} = \eta + i \cdot (\omega \cdot M - S / \omega). \quad (1)$$

In Eq. (1), η is the real (i.e., resistive) part of the impedance and is positive if the cochlea is passive; the imaginary part is seen to involve the surface mass density M and the stiffness S of the BM and the cells attached to it; M includes those elements of the cochlear partition which move “up and down” in a travelling wave (TW) but excludes the liquid particles above and below the partition (which in a TW move on elliptical trajectories in x - z planes).

The “BMR map” is defined to yield, at given x , the resonance frequency f_{res} (BMR) of the local BM resonator [spring constant = $S \cdot dx \cdot dy$; mass = $M \cdot dx \cdot dy$] calculated under the hypothesis that the liquid above and below the partition is absent:

$$f_{res}(\text{BMR}) = [1/(2\pi)] \cdot \sqrt{S/M}. \quad (2)$$

For given x , Eqs. (1) and (2) imply that at the BMR-map frequency f_{res} (BMR) the imaginary part of the local passive BM impedance Z_{BM} vanishes.

The “IOCR map” is defined to yield, at given x , the resonance frequency f_{res} (IOCR) of the local internal organ-of-Corti resonator [spring = OHCs and other nearby structures; angle defined by BM and reticular lamina (RL) varies periodically, as observed, e.g., by Fridberger and Boutet de Monvel (2003)]. The IOCR is thought to represent the second degree of freedom enabling the OHCs to “actively” feed energy into the TW, to thus give rise to the active peak, and to make the resistive impedance (i.e., the real part of $Z_{BM} = \delta p / v_{BM}$) negative. For given x , that real part is therefore conjectured to have its most negative value at the local IOCR-map frequency f_{res} (IOCR); see Fig. 2 below.

2. METHODS

The AP (active peak) map can be determined from experimental below-20-dB curves of BM velocity amplitude versus x or f .

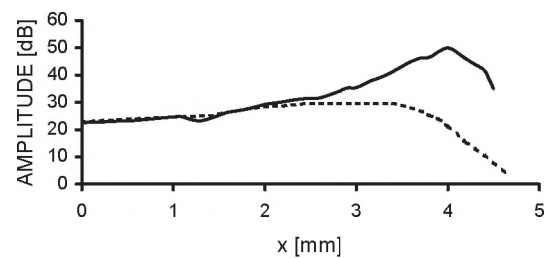


Fig. 1. Experimental BM velocity amplitude (in dB re stapes) versus distance x from stapes; guinea-pig; $f = 17$ kHz; SPL: solid curve 20 dB, dashed curve 100 dB; redrawn from de Boer (2006).

In Fig. 1, e.g. (guinea-pig, 17 kHz), the AP-map place (maximum of solid curve) is seen to be $x(\text{AP}) = 4.0$ mm.

The *PP* (*passive peak*) map can be estimated from experimental healthy-cochlea ~ 100 -dB and post-mortem curves. In Fig. 1, the PP-map place (maximum of dashed curve) is seen to be $x(\text{PP}) \approx 2.8$ mm.

The *IOCR* (*internal organ-of-Corti resonator*) map can be derived from experimental curves of the low-level real part of the BM impedance versus x .

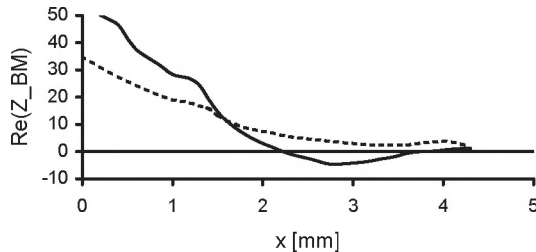


Fig. 2. Real part of the BM impedance (in arbitrary units) versus distance x from stapes; guinea-pig; $f = 17$ kHz; SPL: solid curve 20 dB, dashed curve 100 dB; redrawn from de Boer (2006).

In Fig. 2, e.g. (guinea-pig, 17 kHz), the *IOCR*-map place (i.e., the place of the most negative BM-impedance real part at 20 dB) is seen to be $x(\text{IOCR}) = 2.8$ mm, equal to the *PP*-map place.

In Fig. 2 of de Boer (2006), the *BMR* (*basilar-membrane resonator*) map place (i.e., the zero of the 100-dB imaginary part of the BM impedance for guinea-pig at 17 kHz) is apical of the considered x -range. An extrapolation based on Eqs. (1) and (2) above yields $x(\text{BMR}) = 6$ mm. The guinea-pig map of Greenwood (1990) yields that near the base one octave corresponds to $\Delta x_8 = 2.6$ mm. So $x(\text{BMR}) = 6$ mm is apical of $x(\text{PP}) = x(\text{IOCR}) = 2.8$ mm by 3.2 mm = $1.2 \cdot \Delta x_8$. That *PP*-*BMR* distance of 1.2 octave is confirmed by Figs. 8 and 9 of Kolston (2000) [chinchilla, 10 kHz], and also, in the frequency domain, by Mammano and Ashmore (1993) [guinea-pig, $x = 11$ mm] and by Frosch (2009a,b) [gerbil, $x = 2.4$ mm].

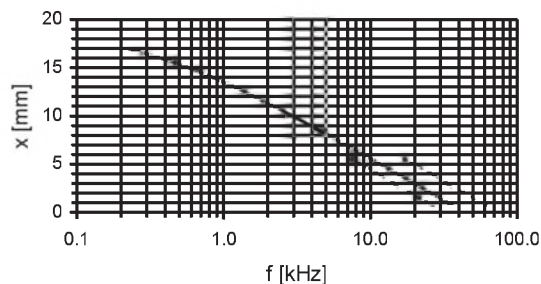


Fig. 3. Maps for guinea pig; $L = 18.5$ mm; solid curve: active-peak (AP) map; lower dashed curve: passive-peak (PP) and internal-organ-of-Corti-resonator (IOCR) maps; upper dashed curve: basilar-membrane-resonator (BMR) map.

3. RESULTS

The guinea-pig maps discussed in Section 2 above are shown in Fig. 3; the active-peak map shown and the mentioned basilar-membrane length, $L = 18.5$ mm, are based on Section IV.A of Greenwood (1990).

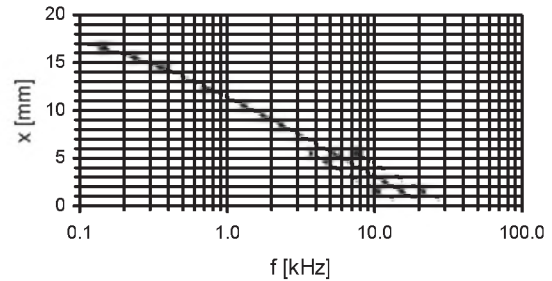


Fig. 4. Same as Fig. 3, for chinchilla; $L = 18.4$ mm.

The chinchilla active-peak map shown in Fig. 4 and the mentioned BM length, $L = 18.4$ mm, are based on Fig. 3 of Greenwood (1990). Further details on the guinea-pig and chinchilla maps, and maps for a third mammalian species (gerbil) are given in Frosch (2009b); the gerbil active-peak map was experimentally determined by Müller (1996).

4. DISCUSSION

A detailed discussion of the “old” and “new” mammalian-cochlea maps introduced above is presented in Frosch (2009b).

REFERENCES

- De Boer, E. (2006). Cochlear Activity in Perspective. In: Nuttall, A. L. et al. (Eds.), *Auditory Mechanisms*. World Scientific, New Jersey, pp. 393-409.
- De Boer, E. (1996). Mechanics of the Cochlea: Modeling Efforts. In: Dallos, P. et al. (Eds.), *The Cochlea*. Springer, New York, pp. 258-317.
- Fridberger, A., Boutet de Monvel, J. (2003). Sound-induced differential motion within the hearing organ. *Nature neurosci.* 6, 446-448.
- Frosch, R. (2009a). DP Phases in Mammalian Cochleae, Predicted from Liquid-Surface-Wave Formulas. In: N.P. Cooper and D.T. Kemp (Eds.), *Concepts and Challenges in the Biophysics of Hearing*, World Scientific, New Jersey, pp. 41-47.
- Frosch, R. (2009b). Old and New Cochlear Maps. Submitted to *Canadian Acoustics*.
- Greenwood, D. D. (1990). A cochlear frequency-position function for several species – 29 years later. *J. Acoust. Soc. Am.* 87, 2592-2605.
- Kolston, P. J. (2000). The importance of phase data and model dimensionality to cochlear mechanics. *Hear. Res.* 145, 25-36.
- Mammano, F., Ashmore, J. F. (1993). Reverse transduction measured in the isolated cochlea by laser Michelson interferometry. *Nature* 365, 838-841.
- Müller, M. (1996). The cochlear place-frequency map of the adult and developing Mongolian gerbil. *Hear Res.* 94, 148-156.